ELSEVIER

Chemical Engineering Journal 77 (2000) 143–151

Chemical Engineering Journal

www.elsevier.com/locate/cej

Modelling sieve tray hydraulics using computational fluid dynamics

J.M. van Baten, R. Krishna *

Department of Chemical Engineering, University of Amsterdam, Nieuwe Achtergracht 166, 1018 WV Amsterdam, The Netherlands

Received 15 April 1999; received in revised form 17 September 1999; accepted 19 September 1999

Abstract

We develop a computational fluid dynamics (CFD) model for describing the hydrodynamics of sieve trays. The gas and liquid phases are modelled in the Eulerian framework as two interpenetrating phases. The interphase momentum exchange (drag) coefficient is estimated using the Bennett et al. (1983) correlation as basis. Several three-dimensional transient simulations were carried out for a 0.3 m diameter sieve tray with varying superfical gas velocity, weir height and liquid weir loads. The simulations were carried out using a commercial code CFX 4.2 of AEA Technology, Harwell, UK and run on a Silicon Graphics Power Challenge workstation with six R10000 200 MHz processors used in parallel. The CFD simulations reflect chaotic tray hydrodynamics and reveal several liquid circulation patterns, which have true three-dimensional character. The clear liquid height determined from these simulations is in good agreement with the Bennett correlation.

It is concluded that CFD can be a powerful tool for modelling and design of sieve trays.

Keywords: Computational fluid dynamics; Sieve trays; Clear liquid height; Froth height; Froth density

1. Introduction

Distillation is the most widely used separation technique and is usually the first choice for separating mixtures. Only when distillation fails does one look for other separation alternatives. One of the major factors that favour distillation is the fact that large diameter columns can be designed and built with confidence. Sieve tray distillation columns are widely used in industrial practice and the description of the hydrodynamics of sieve trays is of great importance. A proper prediction of the sieve tray hydraulics is necessary for the prediction of separation efficiency and overall tray performance. For a given set of operating conditions (gas and liquid loads), tray geometry (column diameter, weir height, weir length, diameter of holes, fractional hole area, active bubbling area, downcomer area) and system properties, it is required to predict the flow regime prevailing on the tray, liquid hold-up, clear liquid height, froth density, interfacial area, pressure drop, liquid entrainment, gas and liquid phase residence time distributions and the mass transfer coefficients in either fluid phase. There are excellent surveys of the published literature in this area [2–6]. Published literature correlations for tray hydrodynamics are largely empirical in nature. In a recent policy document on separations put together by a group of industry and university experts [7], a lack of in-depth understanding of the processes occurring within a distillation column was believed to be a significant barrier to the further improvement of equipment performance. The experts cited transport phenomena such as fluid flow, heat and mass transfer, and multi-phase flow as subjects that are insufficiently understood.

In recent years there has been considerable academic and industrial interest in the use of computational fluid dynamics (CFD) to model two-phase flows in process equipment. The volume-of-fluid (VOF) technique can be used for a priori determination of the morphology and rise characteristics of single bubbles rising in a liquid [8,9]. Considerable progress has been made in CFD modelling of bubbling gas–solid fluidised beds and bubble columns. CFD modelling of fluidised beds usually adopts the Eulerian framework for both the dilute (bubble) and dense phases (emulsion) and makes use of the granular theory to calculate the dense phase rheological parameters [10–18]. The use of CFD models for gas–liquid bubble columns has also evoked considerable interest in recent years and both Euler–Euler and Euler–Lagrange frameworks have been employed for the description of the gas and liquid phases [19–32]. A recent review [33] analyses the various modelling aspects involved for vertical bubble driven flows.

There have been three recent attempts to model tray hydrodynamics using CFD [34–36]. Mehta et al. [34] have

* Corresponding author. Tel.: +31-20-525-7007; fax: +31-20-525-5604.
E-mail address: krishna@chemeng.chem.uva.nl (R. Krishna).

1385-8947/00/$ – see front matter
PII: S1385-8947(99)00164-3

analysed the liquid phase flow patterns on a sieve tray by solving the time-averaged equations of continuity of mass and momentum only for the liquid phase. Interactions with the vapour phase are taken account of by use of interphase momentum transfer coefficients determined from empirical correlations. Yu et al. [35] attempted to model the two-phase flow behaviour using a two-dimensional model, focussing on the description of the hydrodynamics along the liquid flow path, ignoring the variations in the direction of gas flow along the height of the dispersion. Fischer and Quarini [36] have attempted to describe the three-dimensional transient gas–liquid hydrodynamics. An important key assumption made in the simulations of Fischer and Quarini concerns the interphase momentum exchange (drag) coefficient; these authors assumed a constant drag coefficient of 0.44, which is appropriate for uniform bubbly flow. This drag coefficient is not appropriate for description of the hydrodynamics of trays operating in either the froth or spray regimes.

In this paper we develop a three-dimensional transient CFD model, within the two-phase Eulerian framework, to describe the hydrodynamics of a sieve tray. The required interphase momentum exchange coefficient is estimated on the basis of the correlation of Bennett et al. [1] for the liquid hold-up. Simulations have been carried out with varying superficial gas velocity, liquid weir loads and weir heights. The objective of this work is examining the extent to which CFD models can be used as an investigative and design tool in industrial practice. This paper extends our earlier work on CFD modelling of a rectangular sieve tray [37] to columns of circular cross-section.

2. CFD model development

The derivation of the basic equations for dispersed two-phase flows is discussed by Jakobsen et al. [33] and here we present a summary. For either gas (subscript G) or liquid (subscript L) phases in the two-phase dispersion on the tray the volume-averaged mass and momentum conservation equations are given by

$$\frac{\partial(\varepsilon_G\rho_G)}{\partial t} + \nabla\cdot(\rho_G\varepsilon_G\boldsymbol{u}_G) = 0 \tag{1}$$

$$\frac{\partial(\varepsilon_L\rho_L)}{\partial t} + \nabla\cdot(\rho_L\varepsilon_L\boldsymbol{u}_L) = 0 \tag{2}$$

$$\frac{\partial(\rho_G\varepsilon_G\boldsymbol{u}_G)}{\partial t} + \nabla\cdot(\rho_G\varepsilon_G\boldsymbol{u}_G\boldsymbol{u}_G - \mu_G\varepsilon_G(\nabla\boldsymbol{u}_G + (\nabla\boldsymbol{u}_G)^T)) = -\varepsilon_G\nabla p + \boldsymbol{M}_{G,L} + \rho_G\varepsilon_G\boldsymbol{g} \tag{3}$$

$$\frac{\partial(\rho_L\varepsilon_L\boldsymbol{u}_L)}{\partial t} + \nabla\cdot(\rho_L\varepsilon_L\boldsymbol{u}_L\boldsymbol{u}_L - \mu_L\varepsilon_L(\nabla\boldsymbol{u}_L + (\nabla\boldsymbol{u}_L)^T)) = -\varepsilon_L\nabla p - \boldsymbol{M}_{G,L} + \rho_L\varepsilon_L\boldsymbol{g} \tag{4}$$

where ρ_k, $\boldsymbol{u}_k$, e_k and μ_k represent the macroscopic density, velocity, volume fraction and viscosity of the kth phase, respectively, p is the pressure, $\boldsymbol{M}_{G,L}$, the interphase momentum exchange between and liquid phases and $\boldsymbol{g}$ is the gravitational force. The gas and liquid phases share the same pressure field, $p_G=p_L$. The added mass force has been ignored in the present analysis. Lift forces are also ignored in the present analysis because of the uncertainty in assigning values of the lift coefficients to disperse gas phase on a tray. For the continuous, liquid phase, the turbulent contribution to the stress tensor is evaluated by means of k–ε model, using standard single phase parameters C_μ=0.09, $C_{1\varepsilon}$=1.44, $C_{2\varepsilon}$=1.92, σ_k=1 and σ_ε =1.3. No turbulence model is used for calculating the velocity fields within the dispersed gas phase.

For gas–liquid bubbly flows the interphase momentum exchange term is

$$\boldsymbol{M}_{L.G} = \frac{3}{4}\rho_L\frac{\varepsilon_G}{d_G}C_D(\boldsymbol{u}_G - \boldsymbol{u}_L)|\boldsymbol{u}_G - \boldsymbol{u}_L| \tag{5}$$

where C_D is the interphase momentum exchange coefficient or drag coefficient. For the Stokes regime

$$C_D = \frac{24}{Re_G}; \qquad Re_G = \frac{\rho_L U_G d_G}{\mu_L} \tag{6}$$

and for the inertial regime, also known as the turbulent regime

$$C_D = 0.44 \tag{7}$$

which is the relation used by Fischer and Quarini [36]. For the churn-turbulent regime of bubble column operation, Krishna et al. [38] estimated the drag coefficient for a swarm of large bubbles using

$$C_D = \frac{4}{3}\frac{\rho_L - \rho_G}{\rho_L}g d_G\frac{1}{V_{slip}^2} \tag{8}$$

where V_{slip} is the slip velocity of the bubble swarm with respect to the liquid

$$V_{slip} = |\boldsymbol{u}_G - \boldsymbol{u}_L| \tag{9}$$

Substituting Eqs. (8) and (9) into Eq. (5) we find

$$\boldsymbol{M}_{L.G} = \varepsilon_G(\rho_L - \rho_G)g\frac{1}{V_{slip}^2}(\boldsymbol{u}_G - \boldsymbol{u}_L)|\boldsymbol{u}_G - \boldsymbol{u}_L| \tag{10}$$

The slip between gas and liquid can be estimated from superficial gas velocity U_G and the gas hold-up ε_G

$$V_{slip} = \frac{U_G}{\varepsilon_G} \tag{11}$$

In this work we use the Bennett et al. [1] correlation to estimate the gas hold-up:

$$\varepsilon_L^B = \exp\left[-12.55\left(U_G\sqrt{\frac{\rho_{gas}}{\rho_{liq}-\rho_{gas}}}\right)^{0.91}\right]; \qquad \varepsilon_G^B = 1 - \varepsilon_L^B \tag{12}$$

The interphase momentum exchange term is, therefore,

$$\boldsymbol{M}_{\mathrm{L.G}} = \varepsilon_{\mathrm{G}}(\rho_{\mathrm{L}} - \rho_{\mathrm{G}})g\frac{1}{(U_{\mathrm{G}}/\varepsilon_{\mathrm{G}}^{\mathrm{B}})^2}(\boldsymbol{u}_{\mathrm{G}} - \boldsymbol{u}_{\mathrm{L}})|\boldsymbol{u}_{\mathrm{G}} - \boldsymbol{u}_{\mathrm{L}}| \quad (13)$$

This formulation, however, gives numerical difficulties during start-up of the tray with fresh liquid because in the freeboard the liquid hold-up is zero. In order to overcome this problem we modify Eq. (13) as follows

$$\boldsymbol{M}_{\mathrm{L.G}} = \varepsilon_{\mathrm{G}}\varepsilon_{\mathrm{L}}(\rho_{\mathrm{L}} - \rho_{\mathrm{G}})g\left[\frac{1}{(U_{\mathrm{G}}/\varepsilon_{\mathrm{G}}^{\mathrm{B}})^2}\frac{1}{\varepsilon_{\mathrm{L}}^{\mathrm{B}}}\right] \times(\boldsymbol{u}_{\mathrm{G}} - \boldsymbol{u}_{\mathrm{L}})|\boldsymbol{u}_{\mathrm{G}} - \boldsymbol{u}_{\mathrm{L}}| \quad (14)$$

where the term $[1/(U_{\mathrm{G}}/\varepsilon_{\mathrm{G}}^{\mathrm{B}})^2 1/\varepsilon_{\mathrm{L}}^{\mathrm{B}}]$ is estimated a priori from the Bennett relation (12). This approach ensures that the average gas hold-up in the gas–liquid dispersion on the froth conforms to experimental data over a wide range of conditions (as measured by Bennett et al. [1]). When applying incorporating Eq. (14) for the gas–liquid momentum exchange within the momentum balance relations (3) and (4) the local, transient, values of $\boldsymbol{u}_{\mathrm{G}}$, $\boldsymbol{u}_{\mathrm{L}}$, ε_{G} and ε_{L} are used. A further point to note is that use of Eq. (14) for the momentum exchange obviates the need for specifying the bubble size. Indeed for the range of superficial gas velocities used in our simulations we do not expect well-defined bubbles. The two-phase Eulerian simulation approach used here only requires that the gas phase be the dispersed phase; this dispersion could consist of either gas bubbles or gas jets, or a combination thereof.

A commercial CFD package CFX 4.2 of AEA Technology, Harwell, UK, was used to solve the equations of continuity and momentum for the two-fluid mixture. This package is a finite volume solver, using body-fitted grids. The used grid is non-staggered. Discretisation of the equations at the grid is performed using a finite differencing (finite volume) method. Physical space is being mapped to a rectangular computational space. Velocity vector equations are being treated as scalar equations, one scalar equation for each velocity component. All scalar variables are discretised and evaluated at the cell centres. Velocities required at the cell faces are evaluated by applying an improved Rhie–Chow [39] interpolation algorithm. Transport variables such as diffusion coefficients and effective viscosities are evaluated and stored at the cell faces. The pressure–velocity coupling is obtained using the SIMPLEC algorithm [40]. For the convective terms in Eqs. (1)–(4) hybrid differencing was used. No problems with numerical diffusion are anticipated in view of the smallness of the grid and time steps used. A fully implicit backward differencing scheme was used for the time integration. Fig. 1 shows the configuration of the system which has been simulated. The diameter of the tray is 0.3 m with a height of 0.12 m. The length of the weir is 0.18 m, giving a flow path length of 0.24 m. The liquid enters the tray through a rectangular opening which is 0.015 m high. The height of the weir is varied in the simulations and has the values of 60, 80 and 100 mm. The total number of grid cells used in the simulations is $48\times60\times24=69120$; 48 cells in liquid flow direction, 60 cells in direction perpendicular to the liquid flow and 24 cells in the vertical direction. Fig. 2 shows the layout of the distributor grid, which consists of 180 holes. The choice of the grid size is based on our experience gained in the modelling of fluidised beds and gas–liquid bubble columns operating in the churn-turbulent regime [25,26]. The chosen grid size of 5 mm is smaller than the smallest grid used in our earlier study [25,26], where grid convergence was satisfied. The use of warped square holes does not impact on the simulation results because we

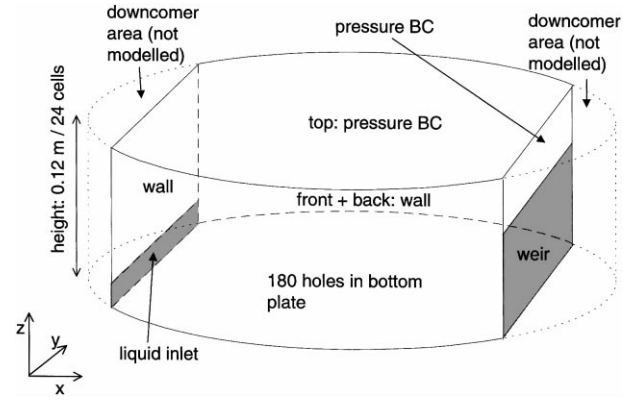

Fig. 1. Specification of the computational space used in the CFD simulations. Total cross-sectional area of column=0.07068 m^2; downcomer area=0.003675 m^2; active bubbling area=0.063 m^2; total number of holes=180; hole area=0.00414 m^2; fractional hole area to bubbling area=6.54%.

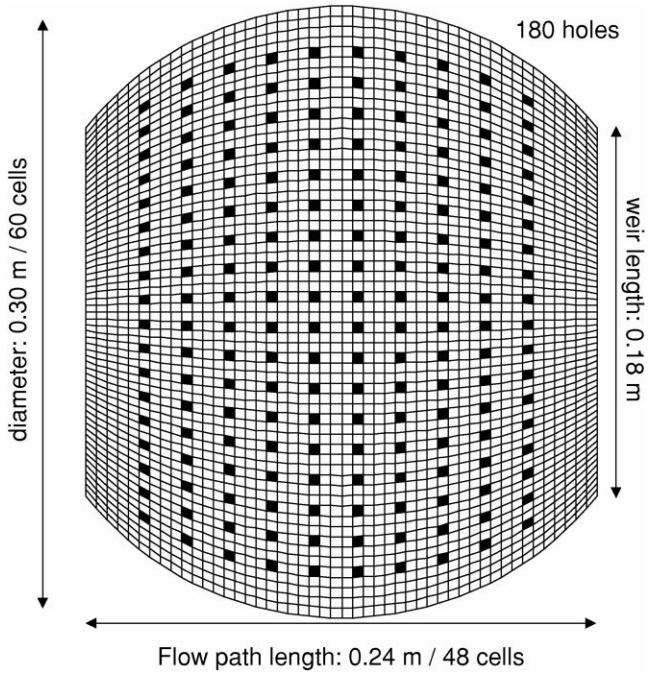

Fig. 2. Layout of the distributor plate used in the CFD simulations: total number of holes=180; hole area=0.00414 m^2; fractional hole area to bubbling area=6.54%.

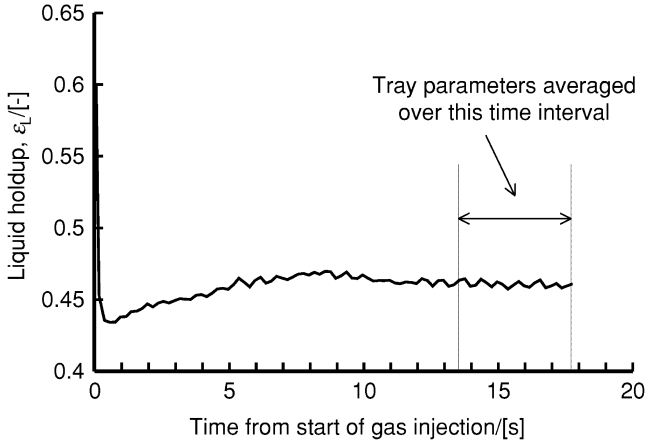

Fig. 3. Transient holdup monitored as a function of time after injection of gas. U_G=0.7 m/s; weir height h_w=80 mm; liquid weir load Q_L/W=1.2×10^{-3} m^3/s/m.

use the Eulerian framework for describing either fluid phase. The geometry of the holes would influence the results in VOF simulations, which is used for a priori prediction of bubble dynamics [8].

Air, at ambient pressure conditions, and water was used as the gas and liquid phases respectively. At the start of a simulation, the tray configuration shown in Fig. 1 is filled with a uniform gas–liquid dispersion, with 10% gas holdup, up to the height of the weir and gas is injected through the holes at the distributor. The time increment used in the simulations is 0.002 s. During the simulation the volume fraction of the liquid phase in the gas–liquid dispersion in the system is monitored and quasi-steady state is assumed to prevail if the value of the hold-up remains constant for a period long enough to determine the time-averaged values of the various parameters. Typically, steady state is achieved in about 15 s from the start of the simulations; see Fig. 3. For obtaining the values of the clear liquid height, gas holdup of dispersion, etc, the parameter values are averaged over a sufficiently long period over which the holdup remains steady (see Fig. 3).

Simulations have been performed on a Silicon Graphics Power Challenge with six R10000 processors running at 200 MHz. A typical simulation took about 4 days to simulate 20 s of tray hydrodynamics. From the simulation results, average liquid hold-up as a function of height has been determined. Dispersion height has been defined by the height at which the average liquid hold-up drops below 10%. Clear liquid height has been determined by multiplying the average liquid hold-up with the height of the computational space (0.12 m). Average liquid hold-up has been calculated by dividing clear liquid height by dispersion height.

Further computational details of the algorithms used, boundary conditions, including animations of two typical simulations, at U_G=0.01 and 0.7 m/s are available on our web site: http://ct-cr4.chem.uva.nl/sievetrayCFD.

3. Simulation results

We first tried to gain an insight into the liquid flow patterns on the tray by simulating a tray at a superficial gas velocity of only 0.01 m/s. The boundary conditions used in the computations prevented weeping of the liquid from the distributor holes. Typical snapshots, taken at four different views of the tray, are shown in Fig. 4. As a guide to the eye, a simplified picture of the liquid circulation patterns is indicated at the bottom of Fig. 4. The liquid circulation cells are clearly visible in the vertical direction in both the front and weir view planes. For the top view at a height 10 mm above the distributor the liquid is drawn inwards towards the centre of the tray. When viewed from the top at a height of 40 mm above the distributor, the liquid recirculation patterns near the curved edges are evident; such circulation patterns have been measured experimentally [35,41].

Fig. 5 shows the corresponding snapshots for a tray operating at U_G=0.7 m/s. The chaotic behaviour can be best appreciated by viewing the animations on our website: http://ct-cr4.chem.uva.nl/sievetrayCFD. Near the bottom of the tray, the liquid is drawn toward the centre and is dragged up vertically by the gas phase. The liquid disengages itself from the dispersed gas phase and travels down the sides, resulting in circulation cells which are evident in both the front and weir views. From the top view the liquid re-circulation patterns are less prominent than in the simulation shown in Fig. 4, which was obtained at very low gas velocity. The fully three-dimensional nature of hydrodynamics is evident, and casts doubts on the applicability of CFD models such as that of Yu et al. [35] in which the liquid flow is assumed to be two-dimensional. The front view and the weir view of this simulation show the existence of just two roll cells. Interestingly, this is in contradiction with the assumption made in the literature when modelling sieve tray hydrodynamics, wherein the existence of multiple cells is assumed; see for example the recent paper by Wijn [42].

Fig. 6 presents typical simulation results for the variation of the liquid hold-up along the height of the dispersion. The values of the hold-up are obtained after averaging along the *x*- and *y*-directions and over a sufficiently long time interval once quasi-steady-state conditions are established. The simulated trends in the liquid hold-up with gas velocity U_G are in line with experimental data [43,5].

Figs. 7, 8 and 9 compare the calculations of the clear liquid height from CFD simulations with the Bennett correlation

$$h_{cl} = \varepsilon_L^B \left[h_w + C \left(\frac{Q_L}{W \varepsilon_L^B} \right)^{0.67} \right];$$
$$C = 0.50 + 0.438 \exp(-137.8 h_w) \quad (15)$$

where $\varepsilon_L^B$is determined from Eq. (12). The values of the clear liquid height from the simulations are obtained after averaging over a sufficiently long time interval once quasi-steady state conditions are established and determining the cumu-

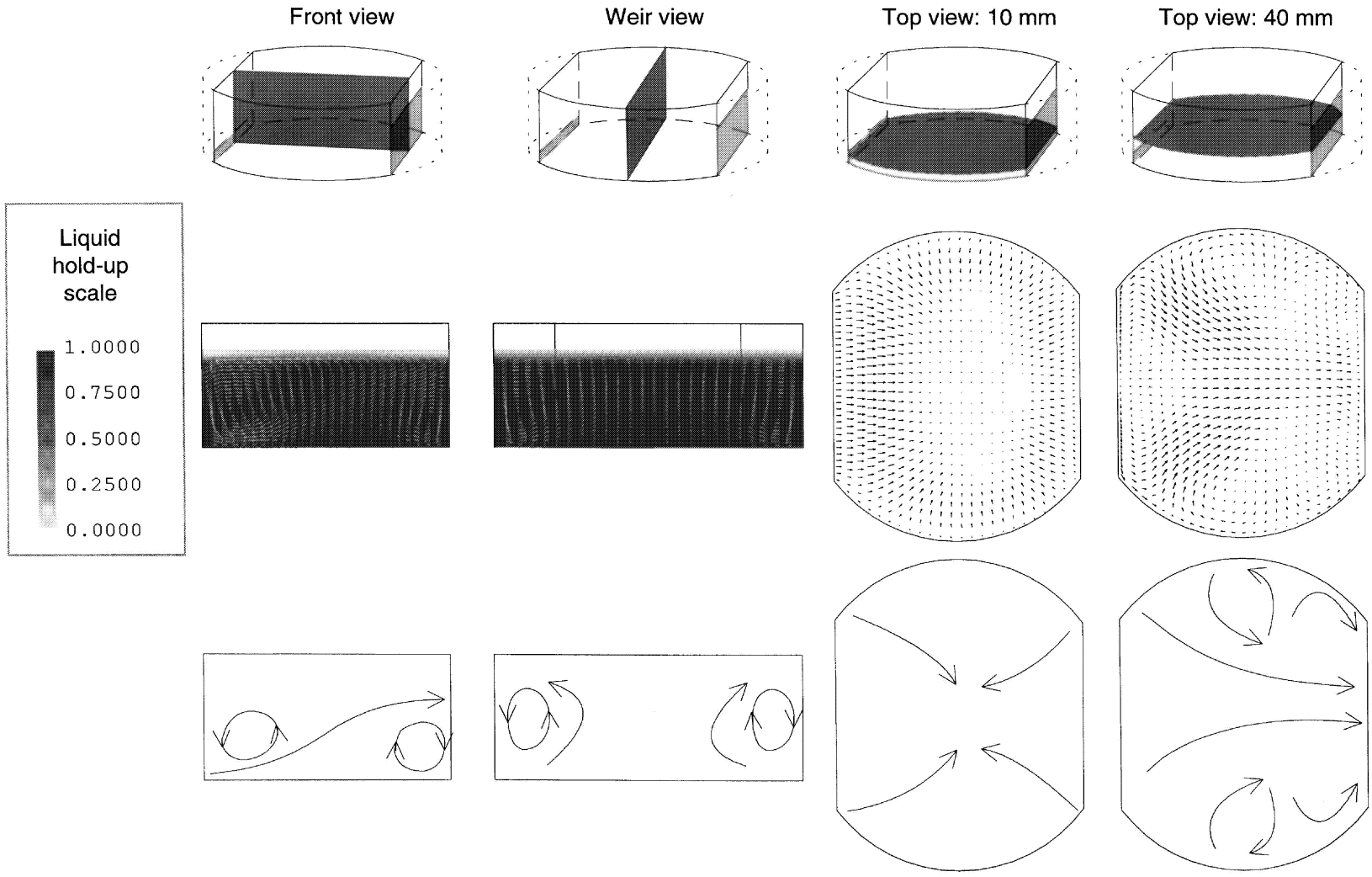

Fig. 4. Snapshots of the front, weir and top views of sieve tray simulations at a superficial gas velocity, U_G=0.01 m/s; weir height h_w=80 mm; liquid weir load Q_L/W=1.2×10^{-3} m^3/s/m. An animation of the simulation can be viewed on our web site: http://ct-cr4.chem.uva.nl/sievetrayCFD.

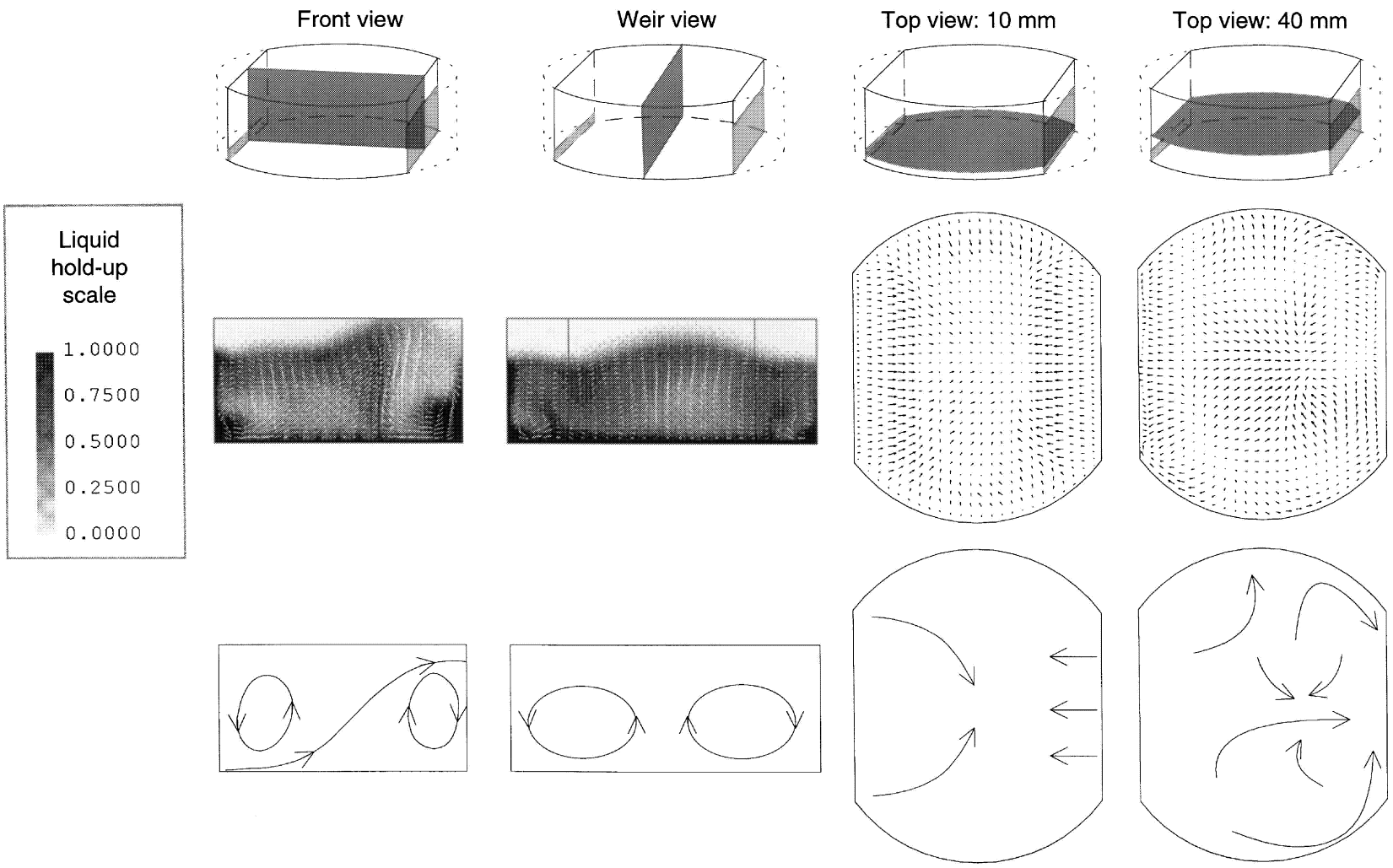

Fig. 5. Snapshots of the front, weir and top views of sieve tray simulations at a superficial gas velocity, U_G=0.7 m/s; weir height h_w=80 mm; liquid weir load $Q_L/W=1.2\times10^{-3}$ m^3/s/m. An animation of the simulation can be viewed on our web site: http://ct-cr4.chem.uva.nl/sievetrayCFD.

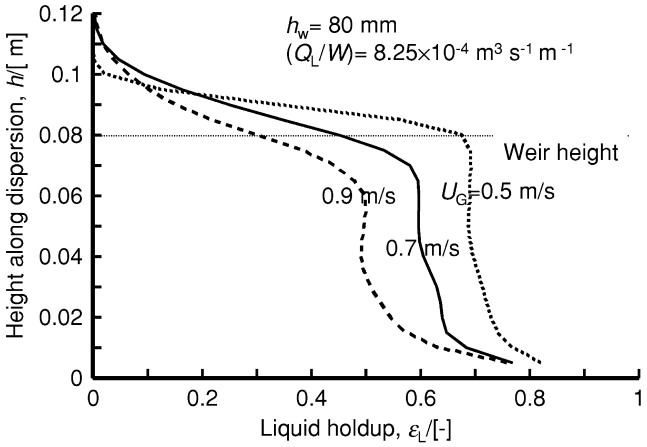

Fig. 6. Distribution of liquid hold-up along the height of the dispersion for superficial gas velocities, U_G=0.5, 0.7 and 0.9 m/s. Weir height h_w=80 mm; liquid weir load Q_L/W=8.25×10^{-4} m^3/s/m. The values of the hold-up are obtained after averaging along the *x*- and *y*-directions and over a sufficiently long time interval once quasi-steady-state conditions are established.

lative liquid hold-up within the computational space. It is remarkable to note that the clear liquid height determined from the CFD simulations match the Bennett correlation quite closely, even though no influence of the weir height or liquid weir load on the interface gas-liquid momentum exchange coefficient has been used in the model. Also shown in Figs. 7, 8 and 9 are the experimental results of Krishna et al. [37] for the clear liquid height obtained in a rectangular sieve tray with 5 mm holes. Both CFD simulations and the Bennett correlation tend to overpredict the clear liquid height. This is because the Bennett correlation was set up for water containing no impurities. It is well known that small impurities tend to prevent coalescence leading to a higher gas holdup with concomitant lower clear liquid height. In order to model non-coalescing systems, appropriate modifications must be made to the interfacial momentum exchange coefficient.

In Figs. 7, 8 and 9 the clear liquid heights were determined by averaging over *x*, *y* and *z* directions of the computational

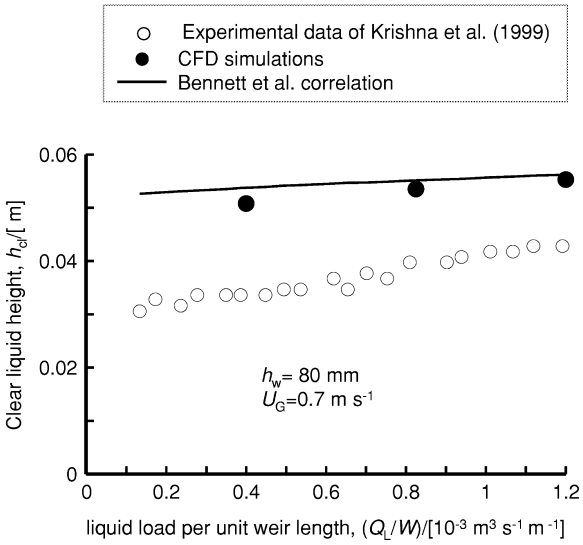

Fig. 8. Clear liquid height as a function of the liquid weir load. Comparison of Bennett correlation with CFD simulation. Weir height h_w=80 mm; Superficial gas velocity U_G=0.7 m/s. The values of the clear liquid height from the simulations are obtained after averaging over a sufficiently long time interval once quasi-steady-state conditions are established and determining the cumulative liquid hold-up within the computational space.

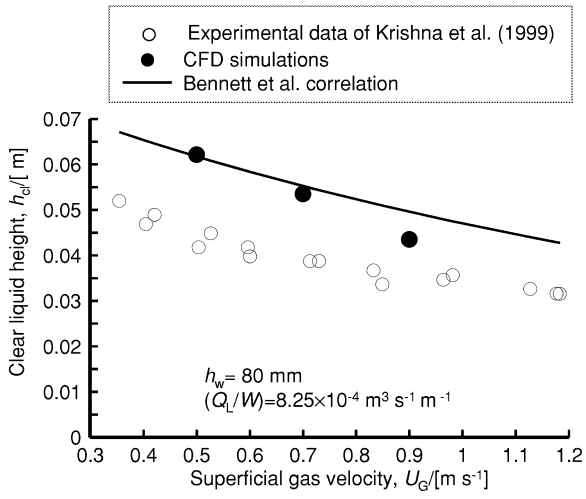

Fig. 7. Clear liquid height as a function of the superficial gas velocity. Comparison of Bennett correlation with CFD simulation. Weir height h_w=80 mm; liquid weir load Q_L/W=8.25×10^{-4} m^3/s/m. The values of the clear liquid height from the simulations are obtained after averaging over a sufficiently long time interval once quasi-steady-state conditions are established and determining the cumulative liquid hold-up within the computational space.

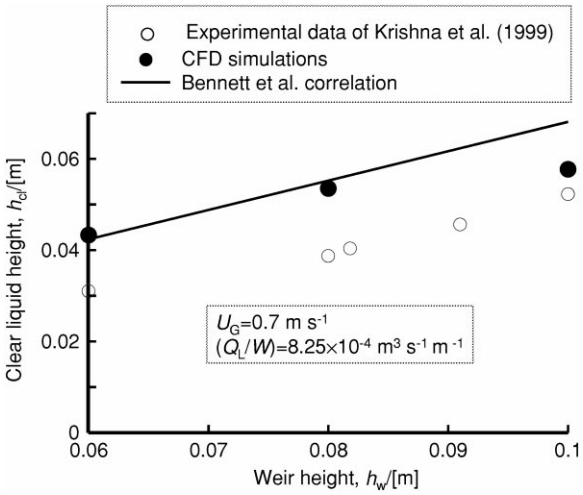

Fig. 9. Clear liquid height as a function of the weir height. Comparison of Bennett correlation with CFD simulation. Q_L/W=8.25×10^{-4} m^3/s/m; Superficial gas velocity U_G=0.7 m/s. The values of the clear liquid height from the simulations are obtained after averaging over a sufficiently long time interval once quasi-steady-state conditions are established and determining the cumulative liquid hold-up within the computational space.

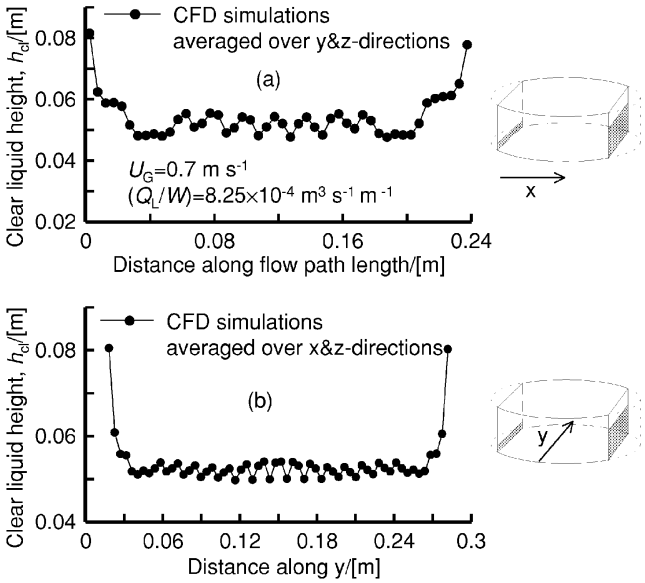

Fig. 10. Clear liquid height along the x- and y-directions. $Q_L/W=8.25\times10^{-4}$ m^3/s/m; $U_G=0.7$ m/s; $h_w=80$ mm. The values of the clear liquid height from the simulations are obtained after averaging over a sufficiently long time interval once quasi-steady-state conditions are established and determining the clear liquid height by averaging over (a) y and z, and (b) over x- and z-directions, respectively.

space. For a typical run, with $Q_L/W=8.25\times10^{-4}$ m^3/s/m, $U_G=0.7$ m/s and $h_w=80$ mm the clear liquid heights in the x- and y-directions are given shown in Fig. 10(a) and (b). The 'bath-tub' profiles of the clear liquid height are clearly evident.

4. Concluding remarks

We have developed a transient three-dimensional CFD model for tray hydrodynamics. The gas and liquid phases are treated as interpenetrating continuous phases and modelled within the Eulerian framework. An important experimental input to the CFD simulations is the slip velocity between the gas and liquid phases; for this purposes the Bennett correlation [1] was used. The tray hydrodynamics has been found to have a true three-dimensional character with liquid circulation cells in both vertical and horizontal directions. The predictions of the clear liquid height and liquid hold-up from the CFD simulations show the right trends with varying superficial gas velocity, liquid weir load and weir height, and match the values of the Bennett correlation quite closely. The important advantage of the CFD simulations is that the influence of tray geometry is automatically taken into account by the code. We conclude that CFD simulations can be a powerful investigative, simulation and design tool for distillation trays.

5. Notation

d_G	diameter of gas bubble, m
C	parameter used in the Bennett correlation (15)
C_D	drag coefficient, dimensionless
g	acceleration due to gravity, 9.81 m/s^2
h_{cl}	clear liquid height, m
h_w	weir height, m
H	dispersion height, m
$\boldsymbol{M}$	interphase momentum exchange term, N/m^3
p	pressure, N/m^2
Q_L	liquid flow rate across tray, m^3/s
Re	Reynolds number, dimensionless
t	time, s
$\boldsymbol{u}$	velocity vector, m/s
U_G	superficial gas velocity, m/s
V_{slip}	slip velocity between gas and liquid, m/s
W	weir length, m
x	coordinate, m
y	coordinate, m
z	coordinate, m

Greek letters

ε	volume fraction of phase, dimensionless
μ	viscosity of phase, Pa s
ρ	density of phases, kg/m^3
τ	stress tensor, N/m^2

Subscripts

cl	clear liquid
disp	dispersion
G	referring to gas phase
k	index referring to one of the three phases
L	referring to liquid phase
slip	slip

Superscripts

B	from Bennett correlation

Acknowledgements

The Netherlands Organisation for Scientific Research (NWO) is gratefully acknowledged for providing financial assistance to J.M. van Baten.

References

[1] D.L. Bennett, R. Agrawal, P.J. Cook, New pressure drop correlation for sieve tray distillation columns, AIChE. J. 29 (1983) 434–442.
[2] J.R. Fair, D.E. Steinmeyer, W.R. Penney, B.B. Croker, Gas absorption and gas–liquid system design, in: D.W. Green, J.O. Maloney (Eds.), Perry's Chemical Engineers' Handbook, 7th Edition, Section 14, McGraw-Hill, New York, 1997.
[3] H.Z. Kister, Distillation Design, McGraw-Hill, New York, 1992.
[4] M.J. Lockett, Distillation Tray Fundamentals, Cambridge University Press, Cambridge, 1986.
[5] F.J. Zuiderweg, Sieve trays. A view on the state of the art, Chem. Eng. Sci. 37 (1982) 1441–1464.
[6] J.G. Stichlmair, J.R. Fair, Distillation Principles and Practice, Wiley-VCH, New York, 1998.
[7] VISION 2020, 1998 Separations Roadmap, Center for waste reduction technologies, AIChE., New York, 1998.
[8] R. Krishna, J.M. Van Baten, Simulating the motion of gas bubbles in a liquid, Nature 398 (1999) 208.
[9] R. Krishna, M.I. Urseanu, J.M. Van Baten, J. Ellenberger, Wall effects on the rise of single gas bubbles in liquids, Int. Commun. Heat Mass Transfer 26 (1999) 781–790.
[10] K.J. Marschall, L. Mleczko, CFD modeling of an internally circulating fluidized-bed reactor, Chem. Eng. Sci. 54 (1999) 2085–2093.
[11] A. Boemer, H. Qi, U. Renz, Eulerian simulation of bubble formation ata jet in a two-dimensional fluidized bed, Int. J. Multiphase Flow 23 (1997) 927–944.
[12] B. Sun, D. Gidaspow, Computation of circulating fluidized-bed riser flow for the fluidization VIII benchmark test, Ind. Eng. Chem. Res. 38 (1999) 787–792.
[13] J. Ding, D. Gidaspow, A bubbling fluidization model using the kinetic theory of granular flow, AIChE. J. 36 (1990) 523–538.
[14] L.S. Fan, C. Zhu, Principles of Gas–Solid Flows, Cambridge University Press, Cambridge, 1998.
[15] G. Ferschneider, P. Mège, Eulerian simulation of dense phase fluidized beds, Revue de L'Institut Français du Pétrole 51 (1996) 301–307.
[16] M. Syamlal, T.J. O'Brien, Computer simulation of bubbles in a fluidized bed, AIChE. Symposium Series No. 270 85 (1989) 22–31.
[17] B.G.M. Van Wachem, J.C. Schouten, R. Krishna, C.M. Van den Bleek, Eulerian simulations of bubbling behaviour in gas-solid fluidized beds, Comput. Chem. Eng. 22 (1998) S299–S306.
[18] B.G.M. Van Wachem, J.C. Schouten, R. Krishna, C.M. Van den Bleek, Validation of the Eulerian simulated dynamic behaviour of gas-solid fluidised beds, Chem. Eng. Sci. 54 (1999) 2141–2149.
[19] N. Boisson, M.R. Malin, Numerical prediction of two-phase flow in bubble columns, Int. J. Numerical Methods in Fluids 23 (1996) 1289–1310.
[20] E. Delnoij, F.A. Lammers, J.A.M. Kuipers, W.P.M. van Swaaij, Dynamic simulation of dispersed gas–liquid two-phase flow using a discreet bubble model, Chem. Eng. Sci. 52 (1997) 1429–1458.
[21] S. Grevskott, B.H. Sannæs, M.P. Dudukovic, K.W. Hjarbo, H.F. Svendsen, Liquid circulation, bubble size distributions, and solids movement in two- and three-phase bubble columns, Chem. Eng. Sci. 51 (1996) 1703–1713.
[22] J. Grienberger, H. Hofmann, Investigations and modelling of bubble columns, Chem. Eng. Sci. 47 (1992) 2215–2220.
[23] R. Krishna, J.M. Van Baten, J. Ellenberger, Scale effects in fluidized multiphase reactors, Powder Technol. 100 (1998) 137–146.
[24] R. Krishna, M.I. Urseanu, J.M. Van Baten, J. Ellenberger, Influence of scale on the hydrodynamics of bubble columns operating in the churn-turbulent regime: experiments vs. Eulerian simulations, Chem. Eng. Sci. 54 (1999) 4903–4911.
[25] A. Lapin, A. Lübbert, Numerical simulation of the dynamics of two-phase gas-liquid flows in bubble columns, Chem. Eng. Sci. 49 (1994) 3661–3674.
[26] T.J. Lin, J. Reese, T. Hong, L.S. Fan, Quantitative analysis and computation of two-dimensional bubble columns, AIChE. J. 42 (1996) 301–318.
[27] A. Sokolichin, G. Eigenberger, Gas–liquid flow in bubble columns and loop reactors: Part I. Detailed modelling and numerical simulation, Chem. Eng. Sci. 49 (1994) 5735–5746.
[28] A. Sokolichin, G. Eigenberger, A. Lapin, A. Lübbert, Direct numerical simulation of gas–liquid two-phase flows. Euler/Euler versus Euler/Lagrange, Chem. Eng. Sci. 52 (1997) 611–626.
[29] R. Torvik, H.F. Svendsen, Modelling of slurry reactors. A fundamental approach, Chem. Eng. Sci. 45 (1990) 2325–2332.
[30] O. Borchersger, C. Busch, A. Sokolichin, G. Eigenberger, Applicability of the standard k–ε turbulence model to the dynamic simulation of bubble columns: part II: comparison of detailed experiments and flow simulations, Chem. Eng. Sci. 54 (1999) 5927–5935.
[31] J. Sanyal, S. Vasquez, S. Roy, M.P. Dudukovic, Numerical simulation of gas–liquid dynamics in cylindrical bubble column reactors, Chem. Eng. Sci. 54 (1999) 5071–5083.
[32] S.S. Thakre, J.B. Joshi, CFD simulation of bubble column reactors: importance of drag force formulation, Chem. Eng. Sci. 54 (1999) 5055–5060.
[33] H.A. Jakobsen, B.H. Sannæs, S. Grevskott, H.F. Svendsen, Modeling of bubble driven vertical flows, Ind. Eng. Chem. Res. 36 (1997) 4052–4074.
[34] B. Mehta, K.T. Chuang, K. Nandakumar, Model for liquid phase flow on sieve trays, Chem. Eng. Res. and Design, Trans. I. Chem. E. 76 (1998) 843–848.
[35] K.T. Yu, X.G. Yan, X.Y. You, F.S. Liu, C.J. Liu, Computational fluid-dynamics and experimental verification of two-phase two-dimensional flow on a sieve column tray, Paper presented at the Working Party meeting on Distillation, Absorption and Extraction, European Federation of Chemical Engineering, Cagliari, 5–7 October 1998.
[36] C.H. Fischer, G.L. Quarini, Three-dimensional heterogeneous modelling of distillation tray hydraulics, Paper presented at the AIChE. annual meeting, 15–20 November 1998, Miami Beach, USA.
[37] R. Krishna, J.M. Van Baten, J. Ellenberger, A.P. Higler, R. Taylor, CFD simulations of sieve tray hydrodynamics, Chem. Eng. Res. Design, Trans. I. Chem. E. 77 (1999) 639–646.
[38] R. Krishna, M.I. Urseanu, J.M. Van Baten, J. Ellenberger, Rise velocity of a swarm of large gas bubbles in liquids, Chem. Eng. Sci. 54 (1999) 171–183.
[39] C.M. Rhie, W.L. Chow, Numerical study of the turbulent flow past an airfoil with trailing edge separation, AIAA J. 21 (1983) 1525–1532.
[40] J. Van Doormal, G.D. Raithby, Enhancement of the SIMPLE method for predicting incompressible flows, Numer. Heat Transfer 7 (1984) 147–163.
[41] K.E. Porter, M.J. Lockett, C.T. Lim, The effect of liquid channelling on distillation plate efficiency, Trans. I. Chem. E. 45 (1972) 91–101.
[42] E.F. Wijn, The effect of downcomer layout pattern on tray efficiency, Chem. Eng. J. 63 (1996) 167–180.
[43] P.A. M, F.J. Zuiderweg, Sieve plates: dispersion density and flow regimes, Inst. Chem. Eng. Symp. 56 (1979) 2.2/1–2.2/26.